A Quantitative Model-Independent Method for Global Sensitivity Analysis of Model Output

Author(s): A. Saltelli, S. Tarantola and K. P.-S. Chan

A Quantitative Model-Independent Method for Global Sensitivity Analysis of Model Output

A. Saltelli, S. Tarantola, and K. P.-S. Chan

Joint Research Centre of the European Commission
21020   Ispra (VA)
Italy
(andrea.saltelli@jrc.it)
(stefano.tarantola@jrc.it)
(karen.chan@jrc.it)

A new method for sensitivity analysis (SA) of model output is introduced. It is based on the Fourier amplitude sensitivity test (FAST) and allows the computation of the total contribution of each input factor to the output's variance. The term "total" here means that the factor's main effect, as well as all the interaction terms involving that factor, are included. Although computationally different, the very same measure of sensitivity is offered by the indices of Sobol'. The main advantages of the extended FAST are its robustness, especially at low sample size, and its computational efficiency. The computational aspects of the extended FAST are described. These include (1) the definition of new sets of parametric equations for the search-curve exploring the input space, (2) the selection of frequencies for the parametric equations, and (3) the procedure adopted to estimate the total contributions. We also address the limitations of other global SA methods and suggest that the total-effect indices are ideally suited to perform a global, quantitative, model-independent sensitivity analysis.

KEY WORDS: Computational model; Fourier amplitude sensitivity test (FAST); Nonlinear and nonmonotonic models; Total sensitivity indices.

1.   INTRODUCTION

The objective of sensitivity analysis (SA) of model output can be defined (loosely) as "to ascertain how a given model (numerical or otherwise) depends on its input factors." Thus, SA can be of use in the growing field of numerical simulation, where mathematical and computational models are used for the study of systems, especially complex ones. SA helps to understand the behavior of a model, the coherence between a model and the world, and how different parts of the model interplay. Beyond these quite general statements about the role of SA lies the large variety of problem settings that may be encountered in actual SA studies (Saltelli and Scott 1997).

In practice two different schools of thought may be identified, the local SA school and the global one. In the first, the local response of the output(s), obtained by varying input factors one at a time, is investigated while holding the others fixed to a central (nominal) value. This involves partial derivatives, possibly normalized by the nominal value of the factor or by its standard deviation. The analysis is run at a given central point in the space of the input factors, and the volume of the region explored is nil. The second SA school is more ambitious in two respects: First, the space of the input factors is explored within a finite (or even infinite) region and, second, the variation of the output induced by a factor is taken globally—that is, averaged over the variation of all the factors.

The local sensitivity school has produced impressive results, especially for the treatment of large systems of differential equations [e.g., see the work on differential analysis and adjoint techniques by the Oak Ridge group in the 80s (Cacuci 1981a,b; Oblow, Pin, and Wright 1986)]. Rabitz (1989) used local SA to correlate quantum mechanic factors to macroscopic observables such as chemical kinetic constants. For a review carefully covering the local SA methods, see Turanyi (1990).

Although local SA and differential analysis are almost synonymous, several different approaches have been attempted for global sensitivity analysis, due to the intrinsic difficulty of building an effective and rigorous measure over a finite space of variation for the inputs. A qualitative type of global SA is that offered by some screening methods, aimed at identifying the active factors of a model at a low computational cost (e.g., see Morris 1991; Saltelli, Andres, and Homma 1995). By using screening methods, factors can be ranked in order of their importance. The percentage of the output variation that each factor is accounting for cannot be quantified, however.

The work of researchers like Iman, Conover, and Helton helped to promote the use of global SA (see Helton 1993 for a review). These investigators have tested robust methods based on Monte Carlo regression and correlation analysis and on the use of scatterplots. Standardized regression coefficients (SRC), correlation measures (Pearson), and partial correlation coefficients (PCC) have been used with some success.

The ordering of importance of the input factors based on these statistics is as good as the associated model coefficient of determination R^2. In other words, the closer R^2 is to 1, the better are the results. When R^2 is lower than 1, say .6 or .8, it implies that there is a fraction of the output variance (40% and 20%, respectively) that is left unaccounted for. This does not imply that the analysis is useless but only that its results cannot be taken as quantitative.

Factors are ranked in order of influence on the output, but their relative weight remains unknown, and perhaps the ranking could change as well if one were capable of attributing the remaining variance to this or that factor. In other words, SRC gives information on the linear regression model that is used to describe the system model, not on the system model itself.

The same authors recommended the use of rank transformed measures [standardized rank regression coefficients (SRRC), Spearman correlation, partial rank correlation coefficients (PRCC)] for nonlinear models. Rank-based methods offer a robust and easy-to-implement SA, provided that the input–output relationship is monotonic.

Rank-transformed statistics only work (high R^2 on the ranks) for monotonic models; moreover, the rank transformation modifies the model under analysis, thus rendering its conclusion even more qualitative (Saltelli, Andres, and Homma 1993; Saltelli and Sobol' 1995).

Nonlinear, nonmonotonic problems are often encountered in everyday model building. These problems call for an SA that is independent from assumptions about the model structure.

The Fourier amplitude sensitivity test (FAST), introduced in the 70s (Cukier, Fortuin, Shuler, Petschek, and Schaibly 1973; Schaibly and Shuler 1973; Cukier, Schaibly, and Shuler 1975; Cukier, Levine, and Shuler 1978) and computationally upgraded by Koda, McRae, and Seinfeld (1979), offers such a method (see Sec. 2). FAST was at the time (and probably still is today) one of the most elegant methods for SA and works for monotonic and nonmonotonic models alike. The core feature of FAST is that the multidimensional space of the input factors is explored by a suitably defined search-curve.

A variation to the basic scheme of FAST is given by the Walsh amplitude sensitivity procedure (WASP, Pierce and Cukier 1981), a method for discrete models in which the factor variation is intrinsically two-valued.

FAST computes the "main effect" contribution of each input factor to the variance of the output, a quantity that later investigators indicated as "importance measure" (Hora and Iman 1986; Ishigami and Homma 1990; Iman and Hora 1990; Saltelli et al. 1993; Homma and Saltelli 1996) or "correlation ratio" (Krzykacz 1990; McKay 1996). As discussed in this article, all these measures estimate the same underlying statistical quantity (i.e., all these methods converge at large sample size). The quantity, in Bayesian notation, is given by

$$\frac{\mathrm{var}_X[E(Y|X)]}{\mathrm{var}(Y)},\qquad(1)$$

where Y denotes the output variable, X denotes an input factor, $E(Y|X)$ denotes the expectation of Y conditional on a fixed value of X, and the variance var_X is taken over all the possible values of X.

The success of a given analysis is empirically evaluated by the sum of these terms: If the sum is high (close to 1), then the analysis is successful (e.g., see Liepmann and Stephanopoulos 1985).

The preceding statistics are usually introduced in the textbooks on design of experiments (DOE; e.g., see Box, Hunter, and Hunter 1978). DOE textbooks also indicate how to compute the so-called interaction effect—that is, the effect due to two factors, say x_1 and x_2, that is not amenable to the linear combination of the effects of x_1 and x_2.

DOE implies the decomposition of the response into terms of increasing dimensionality (main effects, two-way interactions, higher-order interactions). The same decompositions are seen in analysis of variance (ANOVA) studies, the variance being decomposed into partial variances of increasing dimensionality. We shall call these decompositions ANOVA-like, FAST being one of the examples [see Archer, Saltelli, and Sobol' (1997) for a discussion of these decompositions in different settings].

The sensitivity measure of Sobol' (1993), first published in Russian in 1990, is an original extension of DOE to the world of numerical experiments. The indices of Sobol' are superior to FAST in that the computation of the higher interaction terms is allowed and in a way similar to the computation of the main effects. In the measure of Sobol', each effect (main or otherwise) is computed by evaluating a multidimensional integral via the Monte Carlo method.

A paradox seems to emerge when comparing DOE (for physical experiments) with SA (for numerical experiments): In physical experimental design, the variation in the factors is often moderate (due to cost, for instance), and as a result the interaction terms tend to be small. That is, all models tend to be additive over a small interval of factors variation. In numerical experiments, on the other hand, factors are varied generously over orders of magnitude, and the interaction effects can be very significant and even predominant over the main effects. In spite of this obvious remark, in DOE interaction terms are usually dealt with, but in numerical experiments this is seldom, if ever, the case. Exceptions to this are the work of Cotter (1979), Sacks, Welch, Mitchell, and Wynn (1989), and Sobol' (1993). An estimate of interactions was also offered by the screening test proposed by Morris (1991).

One reason for this apparent paradox is perhaps in the number of factors involved. In industrial experiments for process optimization, and in physical experiments aimed at mechanism identification, there are usually fewer factors, and consequently the number of interaction terms is moderate.

In numerical models, however, the tendency is to vary all the factors. The total number of terms involved in a variance decomposition is $2^n - 1$, where n is the number of factors, which can become prohibitive even for moderate values of n. Furthermore, the larger the number of factors, the higher the likelihood of nonnegligible higher-order terms.

This discussion leads to the conclusion that the most rigorous and theoretically sound approach to global SA available today—that based on partial variances and on the decomposition of the output variance into partial variances of increasing dimensionality—is hindered by a dimensionality barrier.

The method of Sobol' can escape the dimensionality curse. This is done by computing, for each of the n system factors, the so-called "Total Sensitivity Index" (S_{Ti}), defined as the sum of all the sensitivity indices involving that factor (Sobol' 1993; Homma and Saltelli 1996). For example, let us suppose that we have only three factors in our model and that we wish to measure the total effect of factor 1 on the output variance; then the S_{T1} is given by

$$S_{T1} = S_1 + S_{12} + S_{13} + S_{123}, \qquad (2)$$

where S_1 is the so-called first-order sensitivity index for factor 1, S_{1j} is the second-order sensitivity index for the couple of factors 1, and $j(\neq 1)$—that is, the interaction between factors 1 and $j(\neq 1)$—and so on.

Total indices are especially suited to apportion the model variation to the input factors in a complete and quantitative fashion (see Fig. 1).

The effectiveness of the Sobol' method is that the S_{Ti} can be computed with just one Monte Carlo integral per factor. A comparison of the Sobol' method against the factorial sampling plan of Morris (1991) was given by Campolongo and Saltelli (1997).

A feature of FAST that is very appealing in the context of numerical experiments is that it appears to be computationally more efficient than Sobol', albeit with some bias problems (Saltelli and Bolado 1998). This would suggest that one should seek a method that would combine FAST better efficiency with Sobol' capacity to compute total effects. Such a method has been developed and its performance assessed in this article. The main objectives of this article are (1) an improvement of the classic (main-effect) FAST method, (2) the development of an extended FAST-based technique to compute the total-effect indices, and (3) a discussion of the relevance of the total indices for modelers.

In Section 2, the fundamentals of the classic FAST are recalled. The definition of a new sampling procedure for FAST is introduced in Section 2.1. A comparison between the classic FAST and the new sampling procedure for the first-order indices is presented in Section 3, and an extension of FAST for total-effect computation is given in Section 4. Two analytic and one numeric simulation studies are presented in Section 5. The conclusions (Sec. 6) highlight the relevance of the total indices and the superiority of the FAST-based implementation, also due to FAST capacity to compute, with the same sample, both the main-effect and the total-effect index for a given factor.

2. REVIEW OF FAST

Let us consider the model $y = f(\mathbf{x})$. The output y is linked through the model f to a set of n input factors $\mathbf{x} = (x_1, x_2, \ldots, x_n)$. Let us assume that the domain of input factors is the unit hypercube

$$K^n = (\mathbf{x} | 0 \leq x_i \leq 1; i = 1, \ldots, n); \qquad (3)$$

y can be obtained either by an analytical representation of f or directly as the output of a computer program (computational model). Let us assume that $\mathbf{x}$ is a random vector with an assumed pdf $P(\mathbf{x}) = P(x_1, x_2, \ldots, x_n)$ even if, actually, the x_i's are not random variables. A summary statistic that will be useful in the following is the rth moment of y:

$$\langle y^{(r)} \rangle = \int_{K^n} f^r(x_1, x_2, \ldots, x_n) P(x_1, x_2, \ldots, x_n) \, d\mathbf{x}. \qquad (4)$$

Cukier et al. (1978) noted that, using multidimensional Fourier transformation of f, it would be possible, in principle, to perform an ANOVA-like decomposition of the variance of y as function of the input $\mathbf{x}$ in order of increasing dimensionality, thus computing main effects and interactions of any order. The computational complexity of a multidimensional frequency decomposition of f led the authors to suggest a monodimensional Fourier decomposition. This is done along a curve exploring the space K^n. The curve is defined by a set of parametric equations,

$$x_i(s) = G_i(\sin \omega_i s), \qquad \forall \, i = 1, 2, \ldots, n, \qquad (5)$$

where s is a scalar variable varying over the range $-\infty < s < +\infty$, G_i are transformation functions whose properties are defined in Section 2.1, and $\{\omega_i\}, \forall \, i = 1, 2, \ldots, n$, is a set of different (angular) frequencies, to be properly selected, associated with each factor.

As s varies, all the factors change simultaneously along a curve that systematically explores K^n. Each x_i oscillates periodically at the corresponding frequency ω_i, whatever G_i is. The output y shows different periodicities combined
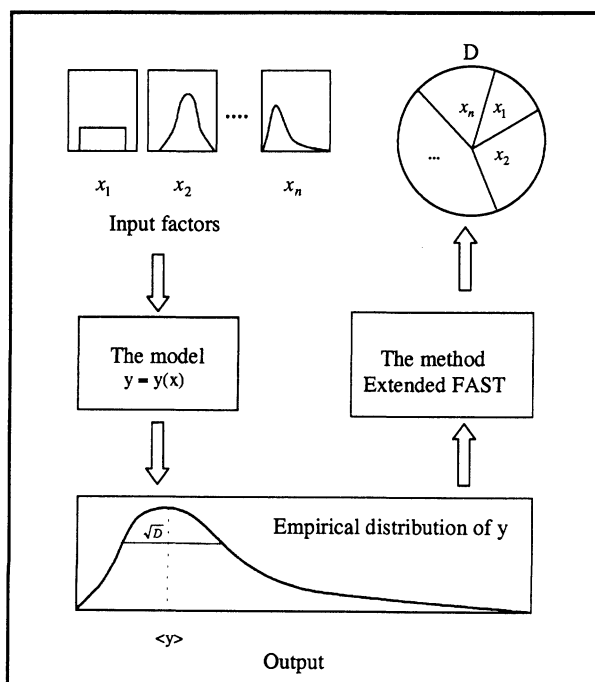

Figure 1. General Scheme of a Quantitative Sensitivity Analysis Method. The total variance of the output is apportioned to the various input factors, as shown by the pie diagram.

with the different frequencies ω_i, whatever the model f is. If the ith factor has strong influence on the output, the oscillations of y at frequency ω_i shall be of high amplitude. This is the basis for computing a sensitivity measure, which is based, for factor x_i, on the coefficients of the corresponding frequency ω_i and its harmonics.

The exploring curve drives arbitrarily close to any point $\mathbf{x}$ of the input domain if and only if the set of frequencies used is incommensurate. To ensure this, none of the frequency must be obtainable as a linear combination of the others with integer coefficients; that is,

$$\sum_{i=1}^{n} r_i \omega_i \neq 0, \qquad -\infty < r_i < +\infty. \qquad (6)$$

In this case we say that the curve is space-filling and, according to the ergodic theorem (Weyl 1938), the quantities in (4) can be computed by evaluating the model along the curve

$$\bar{y}^{(r)} = \lim_{T \to \infty} \frac{1}{2T} \int_{-T}^{T} f^r(x_1(s), x_2(s), \ldots, x_n(s))\, ds - \qquad (7)$$

that is, by a one-dimensional integral. Already, in this equation and in the remainder of the article, we have dropped the pdf's, assuming without loss of generality that all factors are identically and uniformly distributed in the unit cube of Equation (3). Weyl's theorem implies that

$$\langle y^{(r)} \rangle \equiv \bar{y}^{(r)}. \qquad (8)$$

The variance D of the model is

$$D = \langle y^{(2)} \rangle - \langle y^{(1)} \rangle^2 \equiv \bar{y}^{(2)} - (\bar{y}^{(1)})^2 \qquad (9)$$

and can be computed by evaluating one-dimensional integrals as Equation (7).

A space-filling curve is only an idealization because the frequencies $\{\omega_i\}$ cannot be truly incommensurate due to the finite precision of computers. For the computation of main effects, the sets of frequencies recommended by Schaibly and Shuler (1973) have been used.

These sets are commensurate; hence there exists a finite positive rational number T such that $f(s) = f(s + T)$; that is, the curve describes a closed path and Equation (8) no longer holds. For convenience we shall write $f(x_1(s), x_2(s), \ldots, x_n(s))$ as $f(s)$.

Cukier et al. (1973) showed that, if the ω_i's are positive integers, then $T = 2\pi$. By considering $f(s)$ within the finite interval $(-\pi; \pi)$, Equations (7) and (9) become

$$\begin{aligned} \bar{y}^{(r)} &= \frac{1}{2\pi} \int_{-\pi}^{\pi} f^r(s)\, ds \\ \hat{D} &= \bar{y}^{(2)} - (\bar{y}^{(1)})^2 \\ &= \frac{1}{2\pi} \int_{-\pi}^{\pi} f^2(s)\, ds - \left[\frac{1}{2\pi} \int_{-\pi}^{\pi} f(s)\, ds \right]^2. \end{aligned} \qquad (10)$$

We may expand $f(s)$ in a Fourier series

$$y = f(s) = \sum_{j=-\infty}^{+\infty} \{ A_j \cos js + B_j \sin js \}, \qquad (11)$$

where the Fourier coefficients A_j and B_j are defined as

$$\begin{aligned} A_j &= \frac{1}{2\pi} \int_{-\pi}^{\pi} f(s) \cos js\, ds, \\ B_j &= \frac{1}{2\pi} \int_{-\pi}^{\pi} f(s) \sin js\, ds \end{aligned} \qquad (12)$$

over the domain of integer frequencies $j \in \mathcal{Z} = \{-\infty, \ldots, -1, 0, 1, \ldots, +\infty\}$. The spectrum of the Fourier series expansion is defined as $\Lambda_j = A_j^2 + B_j^2$ with $j \in \mathcal{Z}$. Because $f(s)$ is a real-valued function, A_j, B_j, and Λ_j have the following properties: $A_{-j} = A_j, B_{-j} = -B_j, \Lambda_{-j} = \Lambda_j$. By evaluating the spectrum for the fundamental frequency ω_i and its higher harmonics $p\omega_i$, we can estimate D_i—that is, the portion of the output variance D arising from the uncertainty of factor i:

$$\hat{D}_i = \sum_{p \in \mathcal{Z}^o} \Lambda_{p\omega_i} = 2 \sum_{p=1}^{+\infty} \Lambda_{p\omega_i}, \qquad (13)$$

where $\mathcal{Z}^o = \mathcal{Z} - \{0\}$ indicates the set of all relative integer numbers except the 0. The quantity given in (13) is the same as the numerator in (1).

By summing all the $\Lambda_j, j \in \mathcal{Z}^o$, we may estimate the total variance

$$\hat{D} = \sum_{j \in \mathcal{Z}^o} \Lambda_j = 2 \sum_{j=1}^{+\infty} \Lambda_j. \qquad (14)$$

Formulas (10) and (14) provide the same quantity because Parseval's theorem states that

$$\sum_{j \in \mathcal{Z}} \Lambda_j = \frac{1}{2\pi} \int_{-\pi}^{\pi} f^2(s)\, ds = \bar{y}^{(2)}.$$

The ratio $\hat{D}_i / \hat{D}$, denoted by $\hat{S}_i^{\mathrm{FAST}}$, is the needed estimate of the main effect of x_i on y. Its magnitude does not depend, in principle, on the choice of the set of frequencies used in computations.

In Appendix A, the minimum sample size to be used in classic FAST (Cukier et al. 1973) is introduced as

$$N_s = 2M\omega_{\max} + 1, \qquad (15)$$

where M is the interference factor (usually 4 or higher) and $\omega_{\max}$ is the largest among the set of ω_i frequencies.

Other technical details on the computation of FAST are given in Appendixes A–C. These concern the problem of aliasing and interferences and the symmetry properties of $f(s)$.

Saltelli and Bolado (1998) showed that S_i^{FAST} is equivalent to the sensitivity indices of the first order (Sobol' 1993), as well as to other measures proposed by Iman and Hora (1990), Krzykacz (1990), and McKay (1996), all of which can be reconduced to Equation (1). Classic FAST is cheaper to compute than the indices of Sobol' because in FAST a single sample composed, say, of N_s model evaluations can be used for computing all $\hat{S}_i$'s, $i = 1, 2, \ldots, n$, but in Sobol',

a different sample (of size N_s or different) is needed for each $\hat{S}_i$.

For each x_i, the computation of $\hat{D}_i$ involves only the sum of squares of the Fourier coefficients at the fundamental and all the harmonics of ω_i. There are, therefore, several frequencies that are not used for the computation of any of the D_i. These frequencies give information on the interaction effects among factors (see Sec. 4).

2.1 Choice of the Search-Curve

This section discusses the choice of suitable transformations (5), providing a uniformly distributed sample for the factors $x_i, \forall\ i = 1, 2, \ldots, n$, in the unit cube K^n.

Various transformations have been proposed. Cukier et al. (1973) suggested

$$x_i = \bar{x}_i e^{\bar{\nu}_i \sin \omega_i s}, \qquad \forall\ i = 1, \ldots, n, \qquad (16)$$

where $\bar{x}_i$ is the *nominal value* of the ith factor, $\bar{\nu}_i$ defines the endpoints of the estimated range of uncertainty for x_i, and s varies in $(-\pi/2, \pi/2)$.

We plotted Equation (16) with $\bar{\nu}_i = 5, \bar{x}_i = e^{-5}$, and $\omega_i = 11$ in Figure 2(a). A histogram of the empirical distribution of x_i corresponding to this transformation is given in Figure 2(b). This is based on a sample of 89 points chosen at a regular interval along the search-curve s. The histogram appears to be strongly asymmetric because the majority of the sample points lie at the lower end of the dis-

tribution. Clearly this transformation is only suitable for a factor whose pdf is long-tailed and positively skewed.

Later on, Koda et al. (1979) suggested the use of

$$x_i = \bar{x}_i(1 + \bar{\nu}_i \sin \omega_i s), \qquad (17)$$

which has been plotted in Figure 2(c) with $\bar{x}_i = 1/2, \bar{\nu}_i = 1$, and $\omega_i = 11$.

In Figure 2(d), the corresponding histogram with 89 points shows a symmetric U shape. The tails area is highly sampled, but the middle region is poorly represented. Hence, this transformation also fails in providing a sample that is uniformly distributed.

In a review article, Cukier et al. (1978) proposed a general differential form to be solved to deduce the optimal search-curve,

$$\pi(1 - x_i^2)^{1/2} P_i(G_i) \frac{dG_i(x_i)}{dx_i} = 1, \qquad (18)$$

where P_i is the pdf of x_i and is assumed constant in this work.

Here we propose another transformation; namely,

$$x_i = \frac{1}{2} + \frac{1}{\pi} \arcsin(\sin \omega_i s). \qquad (19)$$

This is a set of straight lines oscillating between 0 and 1 [see Fig. 2(e)]. As can be seen in Figure 2(f), the empirical distribution of x_i (with 89 sample points) can be regarded as uniform. Our formula is also a solution of (18).

To illustrate the differences between the transformations in (17) and in (19), we have plotted in Figure 3, (a) and (b), the sample points generated in a case with two factors in which $\{\omega_1, \omega_2\} = \{11, 21\}$. The sample points are more uniformly distributed in the unit square when Formula (19) is used.
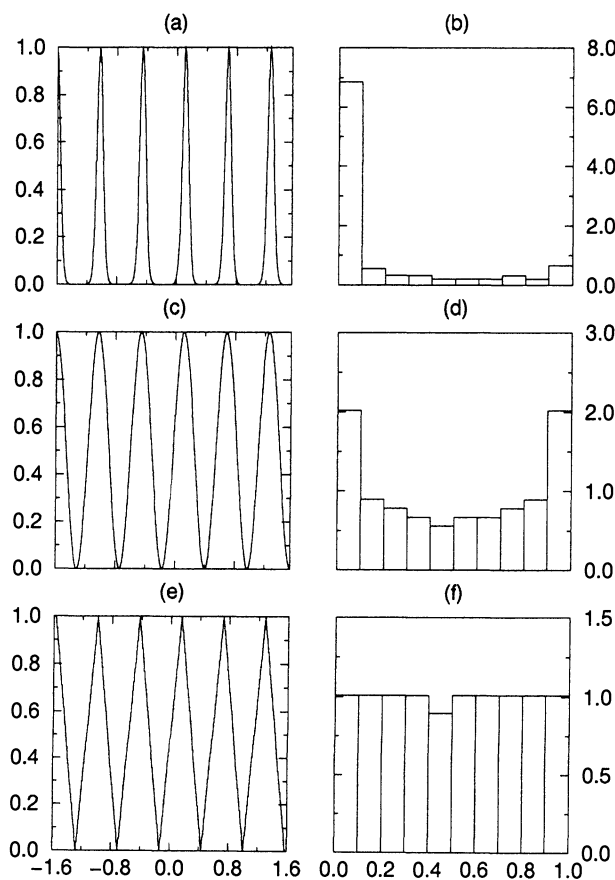
Figure 2. Plot of Three Different Transformations (a), (c), and (e). Their respective empirical distributions are given in (b), (d), and (f).
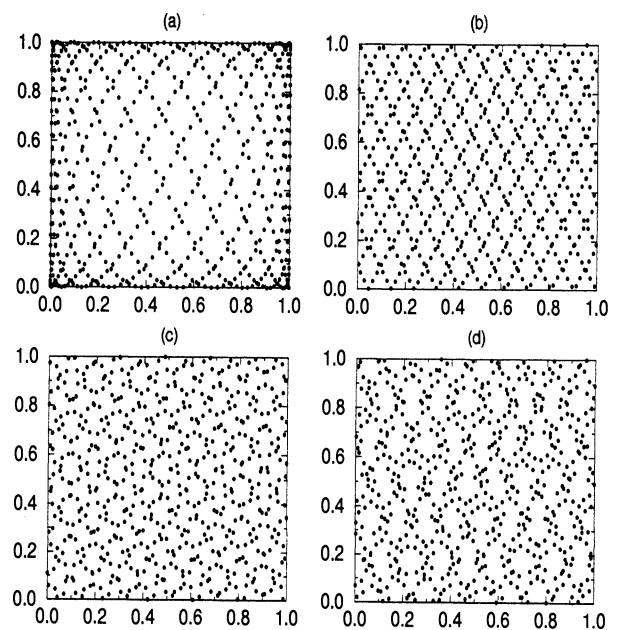
Figure 3. Scatterplots of Sampling Points in a Two-Factors Case Based on (a) the Transformations Given in (17), (b) the Transformations Given in (19), (c) and (d) the Transformations Given in (20) With, Respectively, One and Two Resamplings.

Table 1. Ranges of g_i Function and the Relative Importance of the Corresponding Input Factors x_i's for Some Specific Values of a_i

a_i	Factor x_i	Range of g_i
0	Very important	$0 \leq g_i(x) \leq 2$
1	Important	$.5 \leq g_i(x) \leq 1.5$
9	Unimportant	$.9 \leq g_i(x) \leq 1.1$
99	Nonsignificant	$.99 \leq g_i(x) \leq 1.01$

2.2 Random Phase-shift and Resampling

Here we propose a modification of (19) to obtain a more flexible sampling scheme.

The transformations (16), (17), and (19) have a drawback: They always return the same points in K^n as s varies in $(-\pi/2, \pi/2)$.

To make more efficient use of the model evaluations, we suggest using

$$x_i = \frac{1}{2} + \frac{1}{\pi} \arcsin(\sin(\omega_i s + \varphi_i)), \quad (20)$$

where φ_i is a *random phase-shift* chosen uniformly in $[0, 2\pi)$. The advantage of (20) is that the starting point of the curve can be anywhere within K^n, as shown in Figure 3(c) for the case in which $\{\omega_1, \omega_2\} = \{11, 21\}$. Formula (20) represents the set of equations proposed for the search-curve in K^n.

The symmetry properties of $f(s)$ (see Appendix C) are no longer fulfilled, even if odd frequencies are used, due to the shifting along s introduced by φ_i. The curve must therefore be sampled over $(-\pi, \pi)$. By selecting various sets $\{\varphi_1, \varphi_2, \ldots, \varphi_n\}$, different curves (realizations) can be generated in K^n. Let this procedure be named *resampling*, and let N_r indicate the number of curves used. Figure 3(d) shows an example with $N_r = 2$. In the resampling scheme, the sample size given in (15) must be redefined as

$$N_s = (2M\omega_{\max} + 1)N_r. \quad (21)$$

Formula (21) will be adopted in the rest of this work.

The Fourier analysis is performed independently over each of the N_r curves, obtaining $\hat{D}'_i, \hat{D}''_i, \ldots$ as well as estimates of the total variances $\hat{D}', \hat{D}'', \ldots$. Finally, $\hat{D}_i$ and $\hat{D}$ are obtained by computing the arithmetic means over the N_r estimates.

3. A SIMULATION STUDY: CLASSIC VERSUS EXTENDED FAST

In this section a simulation study is carried out to compare the performances of the extended FAST [using (20)] with those of the previous technique [using (17)]. We use a function introduced by Saltelli and Sobol' (1995), referred to as the *g function* of Sobol':

$$f = \prod_{i=1}^{n} g_i(x_i), \quad (22)$$

where n is the total number of input factors, x_i's, and $g_i(x_i)$ is given by

$$g_i(x_i) = \frac{|4x_i - 2| + a_i}{1 + a_i}$$

$$\text{for} \quad 0 \leq x_i \leq 1 \quad \text{and} \quad a_i \geq 0. \quad (23)$$

This function is relevant to the present investigation because it allows an automatic tuning of the relative importance of factors, as well as of their interactions, by appropriate values of a_i's (see Table 1). It also allows analytic evaluation of the sensitivity indices of any order.

The number of input factors is taken in the range [5, 11]. We consider four cases in which the a_i's are all identically 0s, all 1s, all 9s, and all 99s because the cases in which all the a_i's are equal are the most difficult for SA (Saltelli and Sobol' 1995).

We calculate the first-order indices $\hat{S}_i$ for all cases, as well as the averages over the factors; that is, $\langle \hat{S}_n \rangle = 1/n \sum_{i=1}^{n} \hat{S}_i$. The sample size used in the extended FAST is $N_r(2M\omega_{\max} + 1)$, where M is set to 4 and N_r to 2. The sample size used in the classic FAST is fixed to $4M\omega_{\max} + 1$; that is, it is set to a higher value with respect to the minimum required by the Nyquist criterion (Appendix A). This is done to ensure a fair comparison of the two methods using comparable sample sizes. Table 2 gives the sample sizes and the sets of integer frequencies $\{\omega_i\}$ for $i = 1, 2, \ldots, n$ used in the simulations.

For any given n, all the S_i's are the same because all the a_i's are equal. For the case $a_i = 0$, the averages $\langle \hat{S}_n \rangle$'s obtained from both methods are plotted in Figure 4(a), and the single estimates $\hat{S}_i$'s are shown in Figure 4(b). The estimates from the extended FAST are closer to the analytical values than those obtained by the classic FAST. There is a clear improvement, using the new transformation, when the number of input factors is low, say up to 9. The two methods converge to the analytical values as the sample size increases, following the increase in the number of factors and, hence, in the $\omega_{\max}$ [see Eq. (21)].

Table 2. Number of Input Factors and the Corresponding Sample Sizes and Frequencies Used in the Simulation Study

No. of input factors, n	Sample size N_s	Frequencies $\{\omega_i\}$
5	625	{11, 21, 27, 35, 39}
6	393	{1, 21, 31, 37, 45, 49}
7	697	{17, 39, 59, 69, 75, 83, 87}
8	1,001	{23, 55, 77, 97, 107, 113, 121, 125}
9	1,289	{19, 59, 91, 113, 133, 143, 149, 157, 161}
10	1,641	{25, 63, 103, 135, 157, 177, 187, 193, 201, 205}
11	1,977	{41, 67, 105, 145, 177, 199, 219, 229, 235, 243, 247}

NOTE: $N_s = 4M\omega_{max} + 1$ is the sample size used in the old technique (see Saltelli and Bolado 1998).
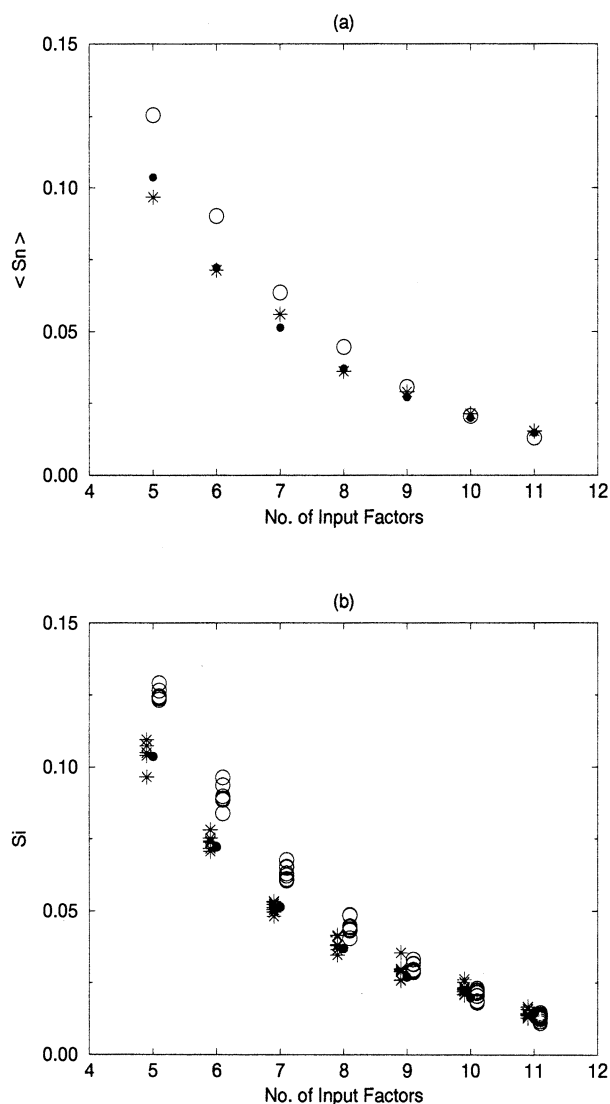
Figure 4. (a) Plot of the Averages $\langle S_n \rangle$'s and (b) Plot of the Single Estimates $\hat{S}_i$, Versus the Number of Input Factors in the Case $a_i = 0$: •, Analytical Value; ○, Old FAST; *, New FAST. In (b), values are slightly shifted sideways.

Similar conclusions can be drawn for the case in which all a_i's are 1s, though the improvement is not so apparent as in the previous case. Results for all unimportant and all nonsignificant factors are not shown because the estimates obtained from both methods and the analytical values are indistinguishable when plotted in the same scale of Figure 4(a). This happens because the output function is rather flat so that the estimates do not depend on uniform or nonuniform sampling.

4. TOTAL–EFFECT INDICES

4.1 The Method

Let us consider the frequencies that do not belong to the set $\{p_1\omega_1, p_2\omega_2, \ldots, p_n\omega_n\}$ with $p_i = 1, 2, \ldots, \infty, \forall i = 1, 2, \ldots, n$. These contain the residual variance $D - \sum_i D_i$ not accounted for by the first-order indices and include interactions among factors of any order.

It would be desirable to identify those frequencies so that the residual variance can be apportioned to the various com-

ponents. This involves the analysis of all the linear combinations among the ω_i's, however, and the complexity of this task is the main reason Fourier analysis of the higher-order terms has never been exploited.

In this chapter, we propose an extension of FAST to estimate the total (all-effects) contribution of each factor to the output variance, as in Equation (2). The computation of the S_{Ti}'s does not give a complete characterization of the system because this could only be achieved by computing all the $2^n - 1$ sensitivity indices. Nevertheless, it allows a full quantification of the importance of each x_i.

We proceed by assigning a frequency ω_i for the ith factor and a different frequency value $\omega_{(i')}$ to all the remaining factors. Thus, by evaluating the spectrum at the frequency $\omega_{(i')}$ and higher harmonics $p\omega_{(i')}$, we can estimate the partial variance $D_{(-i)}$, where the index $-i$ stands for "all but i"—that is, complementary to i—and the $\hat{D}_{(-i)}$ now includes all effects of any order that do not include the factor i. Similarly, $\hat{D}_i$ is obtained by using Equation (13). The total variance is computed as before from Equation (10).

Exactly as in the case of Sobol' indices, we can now estimate D_{Ti} from the variance of the complementary set $D_{(-i)}$ because $D_{Ti} = D - D_{(-i)}$ (Homma and Saltelli 1996). This approach has two advantages: First, for each factor i, we only need to choose two values for the frequencies, ω_i for the factor i and $\omega_{(i')}$ for the complementary set, whatever the number of factors. Second, the problem of interference is eliminated because we can always find a couple of frequencies that do not interfere up to an arbitrarily high M (Appendix B).

The most intuitive choice for the frequencies is to assign a high value to ω_i and a low one to $\omega_{(i')}$, the best possible value for $\omega_{(i')}$ being 1. In fact this latter assumption, though viable, is not the recommended one, as discussed in Section 4.2, but it will be kept as valid for the purpose of the present section.

Let us consider in Figure 5, as an example, an artificial spectrum with $\omega_i = 20$ and $\omega_{(i')} = 1$. Let us note that the components at $\{p\omega_i\} = \{20, 40, 60, \ldots\}$ contribute to D_i and decrease rapidly in amplitude as p increases. The partial
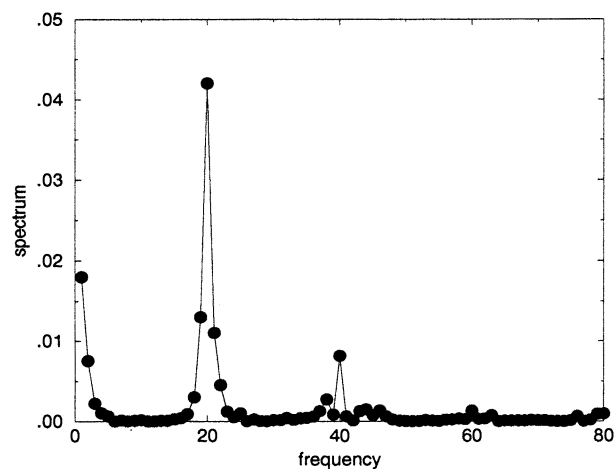

Figure 5. Plot of an Artificial Spectrum in a Typical Configuration with $\omega_i = 20$ and $\omega_{(-i)} = 1$.

variance $D_{(-i)}$ of the $x_{(-i)}$'s can be estimated from the first few spectral components (because the higher harmonics of $\omega_{(i')} = 1$ are 2, 3, 4, ... and usually converge to 0 after a few terms). If this were not the case, we could still obtain good estimates for $D_{(-i)}$ by including more terms in the summation (in this example we could easily consider the first 15 components).

Finally, the information about the term $D_{i(-i)}$, representing the interaction between x_i and $\mathbf{x}_{-i}$, can be read at all the other frequencies in $[1, M\omega_{\max}]$. In particular, it is concentrated around each of the $p\omega_i$'s for $p = 1, 2, \ldots M$.

Figure 5 shows that the spectral components related to $D_{(-i)}$ and $D_{i(-i)}$ in the range $[1, 20]$ are well separated and have similar widths. If some overlaps were to occur, then a higher value for ω_i should be used.

Let us assume, for example, that there is no further information contributing to $D_{(-i)}$ after the frequency 4, having selected 1 as $\omega_{i'}$. Then we are quite sure that an overlap between $D_{(-i)}$ and $D_{i(-i)}$ will not occur if we choose ω_i to be greater than 8. Indeed, with $\omega_i = 9$ we are at the safe side because at frequencies 1, 2, 3, and 4 we have all the information about $D_{(-i)}$ and at frequencies 5, 6, 7, and 8 we have part of the contribution to $D_{i(-i)}$. Thus, the procedure of computing $\hat{D}_{(-i)}$ for the ith factor can be automated by adding all the spectral components in the frequency range $[1, \omega_i/2]$ to avoid the potential overlap region.

So far we have detailed an approach to compute S_{Ti} for a given factor i. What strategy should then be adopted to compute the full set of $S_{Ti}, \forall i = 1, \ldots, n$?

In principle we could select $\omega_{(i')} = 1$, as said before, and the same ω_i for all i's (see Sec. 4.2). Note that a new set (sample) of model evaluations will be needed to evaluate each of the $S_{Ti}, \forall i = 1, \ldots, n$. Thus, we have lost one of the attractive features of the FAST method, that all indices were computed from a single curve; this was the price paid to capture the total effect terms.

The total number of model evaluations required for a complete SA—that is, the computational cost C of the analysis—is, hence,

$$C = nN_r(2M\omega_{\max} + 1), \qquad (24)$$

where $\omega_{\max} = \max\{\omega_i, \omega_{i'}\} \equiv \omega_i$.

4.2 Selection of the Frequencies

We shall rediscuss here the assumption $\omega_{(i')} = 1$. Imagine that two factors x_{i_1} and x_{i_2} belong to the complementary set x_{-i}, for which the same frequency $\omega_{(i')} = 1$ is taken. We show an example with $N_r = 2, M = 4$, and $\omega_i = 20$.

A plot of the two sampling curves in the two-dimensional space (x_{i_1}, x_{i_2}) with 161 points per curve is given in Figure 6(a). Each curve describes a squared trajectory starting and ending at the same random point. This trajectory hits the boundary of the subspace (x_{i_1}, x_{i_2}) at an angle of exactly $45°$, and both x_{i_1} and x_{i_2} make one complete oscillation inside their ranges as s varies in $(-\pi, \pi)$.
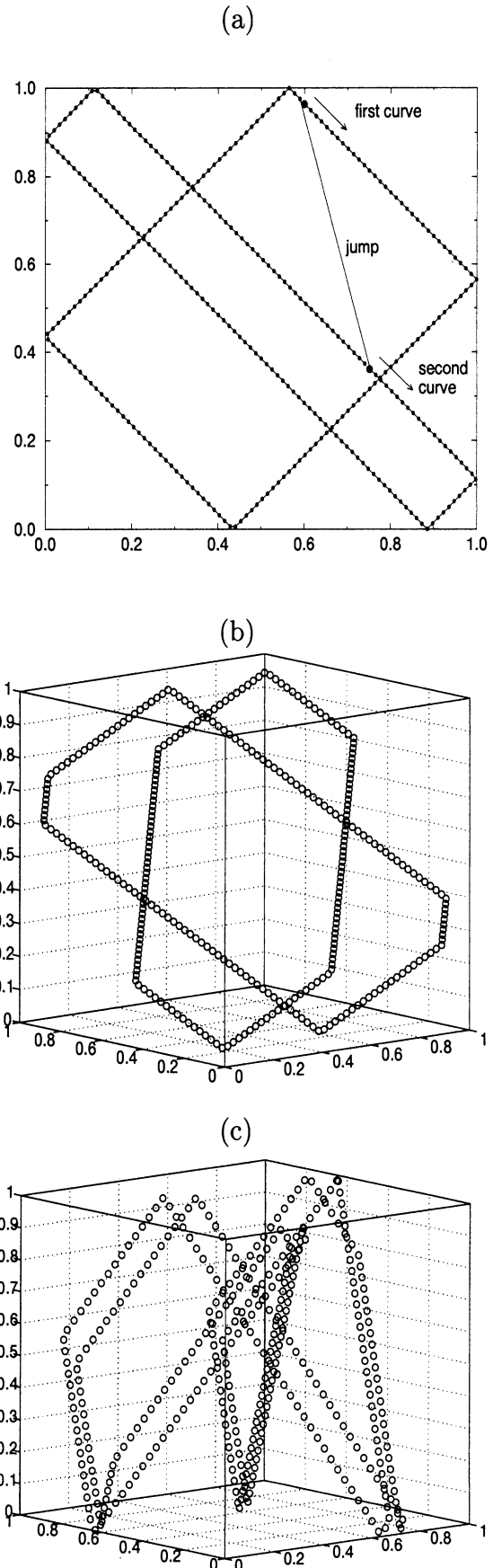
Figure 6. Plot of a Sampling Curve (a) in a Two-Dimensional Subspace, (b) and (c) in a Three-Dimensional Subspace.

Table 3. Sets of Frequencies $\omega_{(-i)}$ Obtained by Using the Criterion Described in this Section for an Eight-Factors Case at Different Sample Sizes

N_s	ω_i	$max\{\omega_{(-i)}\}$	Step	ω_1	ω_2	ω_3	ω_4	ω_5	ω_6	ω_7	ω_8
65	8	1	0	1	1	1	8	1	1	1	1
129	16	2	1	1	2	1	16	1	2	1	2
257	32	4	1	1	2	3	32	1	2	3	4
513	64	8	1	1	2	3	64	5	6	7	8
1,025	128	16	2	1	3	5	128	9	11	13	15
2,049	256	32	4	1	5	9	256	17	21	25	29
4,097	512	64	8	1	9	17	512	33	41	49	57
8,193	1024	128	16	1	17	33	1024	65	81	97	113

NOTE: The assumed factor of interest is the fourth (i.e., $\omega_i = \omega_4$).

Figure 6(a) is an orthogonal projection over (x_{i_1}, x_{i_2}) of what happens in the whole K^n. If we could see the same curves going through the full complementary space x_{-i}, we would see a very sparse space-filling curve; see Figure 6(b) for the case in which the complementary space is simply three-dimensional.

A better coverage of K^3 can be obtained by using a different strategy—that is, by adopting different frequencies for the factors in the complementary set. Let us indicate these frequencies as $\{\omega_{(-i)}\} \equiv \{\omega_{(i')}, \omega_{(i'')}, \omega_{(i''')}, \ldots\}$.

These frequencies must be very similar and, in any case, much lower than the ω_i. In the three-dimensional case, by selecting $\omega_{(i')} = 1, \omega_{(i'')} = 2$, and $\omega_{(i''')} = 3$, we have obtained a better scanning of K^3 [see Fig. 6(c)] at no extra computational cost because the number of model evaluations is dictated by the highest frequency, $\omega_i = 20$ in this case.

To make a different example, in a case with eight factors we could use, alternatively, for the complementary factors, two sets of frequencies:

1. $\{\omega_{(-i)}\} = \{1, 2, 3, 4, 5, 6, 7\}$, with step = 1 between frequencies.
2. $\{\omega_{(-i)}\} = \{1, 3, 5, 7, 9, 11, 13\}$, with step = 2.

The spread of the spectral components that contribute to the complementary variance $D_{(-i)}$ increases as the frequency step increases. In the two cases, we have (1) spread = $M \times max\{\omega_{(-i)}\} = 28$, as $M = 4$ and $max\{\omega_{(-i)}\}$ is 7, and (2) spread = 52.

The larger the spread, the higher is the probability that an unwanted overlap with upper frequencies occurs. To avoid this, a larger value for ω_i must be selected. For the previous example, we should have at least $\omega_i = 2\times$ spread = 56 and at least $\omega_i = 2\times$ spread = 104. To limit the sample size and, at the same time, avoid overlap, we adopt the strategy of assigning the same frequency twice (i.e., to two different factors) or more. In the two cases we would have $\{\omega_{(-i)}\} = \{1, 2, 3, 4, 1, 2, 3\}$ and $\{\omega_{(-i)}\} = \{1, 3, 5, 7, 1, 3, 5\}$. By so doing, $max\{\omega_{(-i)}\}$ is roughly halved. A same frequency is now assigned to two factors of the subset $x_{(-i)}$.

An automated algorithm has been implemented to select the preceding frequencies. The algorithm is structured as follows:

1.   The maximum allowable frequency for the complementary set is given by $max\{\omega_{(-i)}\} = (1/M)(\omega_i/2)$—that is, $1/M$ of the whole spread of the spectrum of the $x_{(-i)}$.
2.   The other frequencies for the complementary set are chosen to exhaust the whole range between 1 and $max\{\omega_{(-i)}\}$, and according to the two following conflicting requirements (1) the step between frequencies must be as large as possible and (2) the number of factors to which the same frequency is assigned must be as low as possible.

Let us refer to Table 3 to illustrate the algorithm for an eight-dimensional problem, where x_4 is the factor of interest. In the first three rows—that is, at low sample size—the maximum value of the complementary frequency is 1, 2, and 4, respectively.

These values are all lower than the number of factors in the complementary set (i.e., 7). This means that it is necessary to assign the same frequency to more than one factor. This is no longer the case at larger sample sizes (4th row onward), where the maximum value for the frequency of the complementary set (8, 16, 32, ...) is bigger than 7 and we are allowed to use different values for all frequencies in the complementary set.

The preceding implies that $N_s = 65$ is a lower bound imposed by $\omega_i = 8$. Lower values of ω_i are not advisable.

4.3   Optimizing the Number of Resamplings N_r and the Frequency ω_i for a Given Sample Size N_s

For a given N_s, the recommended values for ω_i—the frequency assigned to the factor of interest—and for the number of repetitions N_r can be chosen according to Figure 7. Within the suggested region the ratio ω_i/N_r varies between 16 and 64 and all the possible choices are equivalent for a given N_s. The rationale behind the suggestion of Figure 7 is a balance between the values for ω_i and N_r:

1.   If ω_i is low and N_r is high, the sampling over each curve is too sparse.
2.   A high value for ω_i and a low value for N_r imply a too dense sampling over a small number of closed paths.

The optimal region is hence in between, as shown in Figure 7, and the recommended boundaries were determined empirically.
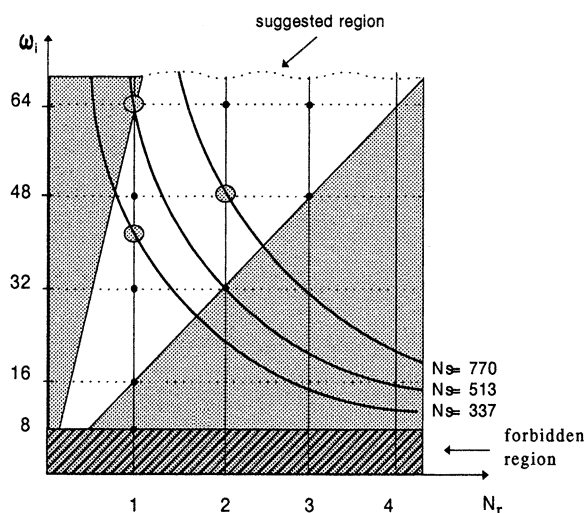
Figure 7. Plot of ω_{max} Against N_r at Different Values of N_s. The recommended values for ω_i and N_r for a given N_s are those lying inside the conic region. The shaded region is allowed but not recommended. The constraints are that ω_i must be greater than or equal to 8 and that N_r is an integer.

When using very low sample sizes, we could be forced to select values lying outside the recommended region. For example $N_s = 65$ implies $N_r = 1$ and $\omega_i = 8$ as discussed in the previous section.

In summary, once the investigator has provided the number of factors n, the sample size N_s, and the interference factor M, the rule illustrated in Figure 7 and the algorithm for the choice of the complementary frequencies (Sec. 4.2) can be employed. These have been adopted systematically in the simulation studies described throughout the rest of this article.

5. SIMULATION STUDIES: TOTAL EFFECT—FAST VERSUS SOBOL'

In this section a comparison between the extended FAST and the method of Sobol' for total sensitivity estimates is illustrated on two simulation studies. The comparison is aimed at low sample sizes. At large ones, Sobol' and FAST estimates converge to the analytical values, although Sobol' is computationally more expensive in terms of number of model evaluations.

The simulation studies are based on two analytic functions, the g function introduced in Section 3 and the Legendre polynomial, as well as on a numerical test case, the Level E, derived from nuclear safety studies. Although the analytical test cases have been selected on purpose because of their nonnegligible interaction terms, the Level E test case can be considered as representative of a large class of physicochemical processes—that is, all those involving mass transfer with chemical reaction.

5.1 Test Case 1

The first test function is the g function of Sobol' described in Section 3. The number of input factors has been set to 8. Four sets (A, B, C, and D) of values for the a_i's are chosen (Table 4). Both the sets A and B represent the extreme case in which all input factors are equally important.

Case A corresponds to the most nonmonotonic case. Case B is still nonmonotonic, but y is a weak function of the x_i's. In set C the factors are in order of decreasing importance, and set D is an example of factors in random order of importance. The analytical values of the S_{Ti}'s are shown in Table 4.

In all the four cases, the method of Sobol' has been performed at sample size N_s equal to 64, 128, 256, 512, and 1,024. Very similar values have been adopted for the extended FAST.

The robustness of the extended FAST is investigated by repeating the experiment N_{rep} times for each of the four cases and at each sample size. For the extended FAST, generating N_{rep} samples is straightforward: A different starting point of the space-filling curve for each replicate can be chosen using the random phase-shift procedure (see Sec. 2.2). For the method of Sobol', described by Sobol' (1993), the only way to randomize is to permute the columns of a random data matrix used as input. In this test case we have 8! possible permutations and we randomly select N_{rep} from these. In cases A and B the a_i's coefficients [Eq. (23)] are all equal so that the number of replicates that can be generated is limited to 8. In cases C and D, N_{rep} is taken to be 100.

The comparisons between the two methods are based on the total absolute error (TAE); namely,

$$\text{TAE} = \sum_{i=1}^{n} |\widehat{S_{Ti}} - S_{Ti}|. \tag{25}$$

The arithmetic means and the standard deviations of these N_{rep} TAE's are computed and are plotted against the sample sizes in Figure 8; the standard deviations are presented as error bars.

For all four cases and for both methods, the means of the TAE's decrease and the error bars become narrower as the sample size increases. In general, the Sobol' estimates present wider error bars than FAST. In cases A, C, and D, FAST performs better than Sobol'. In case B, in which all the factors have weak influence on y, the method of Sobol' gives better results. As noted in Section 3, cases A and B are difficult tests for SA, which explains why the TAE's are higher for these cases than for cases C and D.

5.2 Test Case 2

The second analytical test function is based on the Legendre polynomials of order d, denoted by $L_d(x)$ (Abramowitz and Stegun 1970). The test case was suggested by McKay (1996). We use this test function also to investigate the sensitivity of the new FAST computation to the Nyquist criterion, as well as comparing its performance with that of Sobol'. The model $L_d(x)$ has two input factors: x is uniformly distributed in $[-1, +1]$ and d is a discrete uniformly distributed variable in $[1, 5]$.

The analytical values of the partial variances D_d, D_x, are given in Table 5, as well as the total partial variances computed as

$$D_{Td} = D - D_x \tag{26}$$

Table 4. Choice of a_i Values for the g Function as Described in Section 3 and the Corresponding Analytical Values of S_{Ti}'s for the Input Factors x_i's

Case	a_i for $i = 1, 2, \cdots, 8$	Analytical value of S_{Ti}
A	$0 \ \forall i$	$.278 \ \forall i$
B	$99 \ \forall i$	$.125 \ \forall i$
C	$\{0, 1, 4.5, 9, 99, 99, 99, 99\}$	$\{.787, .242, .034, .010, 1.05 \times 10^{-4}, 1.05 \times 10^{-4}, 1.05 \times 10^{-4}, 1.05 \times 10^{-4}\}$
D	$\{99, 0, 9, 0, 99, 4.5, 1, 99\}$	$\{6.82 \times 10^{-5}, .512, .007, .512, 6.82 \times 10^{-5}, .022, .158, 6.82 \times 10^{-5}\}$

and

$$D_{Tx} = D - D_d. \qquad (27)$$

The corresponding sensitivity indices are shown in bold. Given that the model has two input factors, only two repli-

cates are possible using the method of Sobol'. To assess the robustness of Sobol' estimates, the bootstrap technique has been employed. At any given sample size in the range explored, 100 bootstrap replicas of the sample have been obtained, providing 100 bootstrap estimates of S_{Ti}. The arithmetic mean and the range (minimum and maximum)
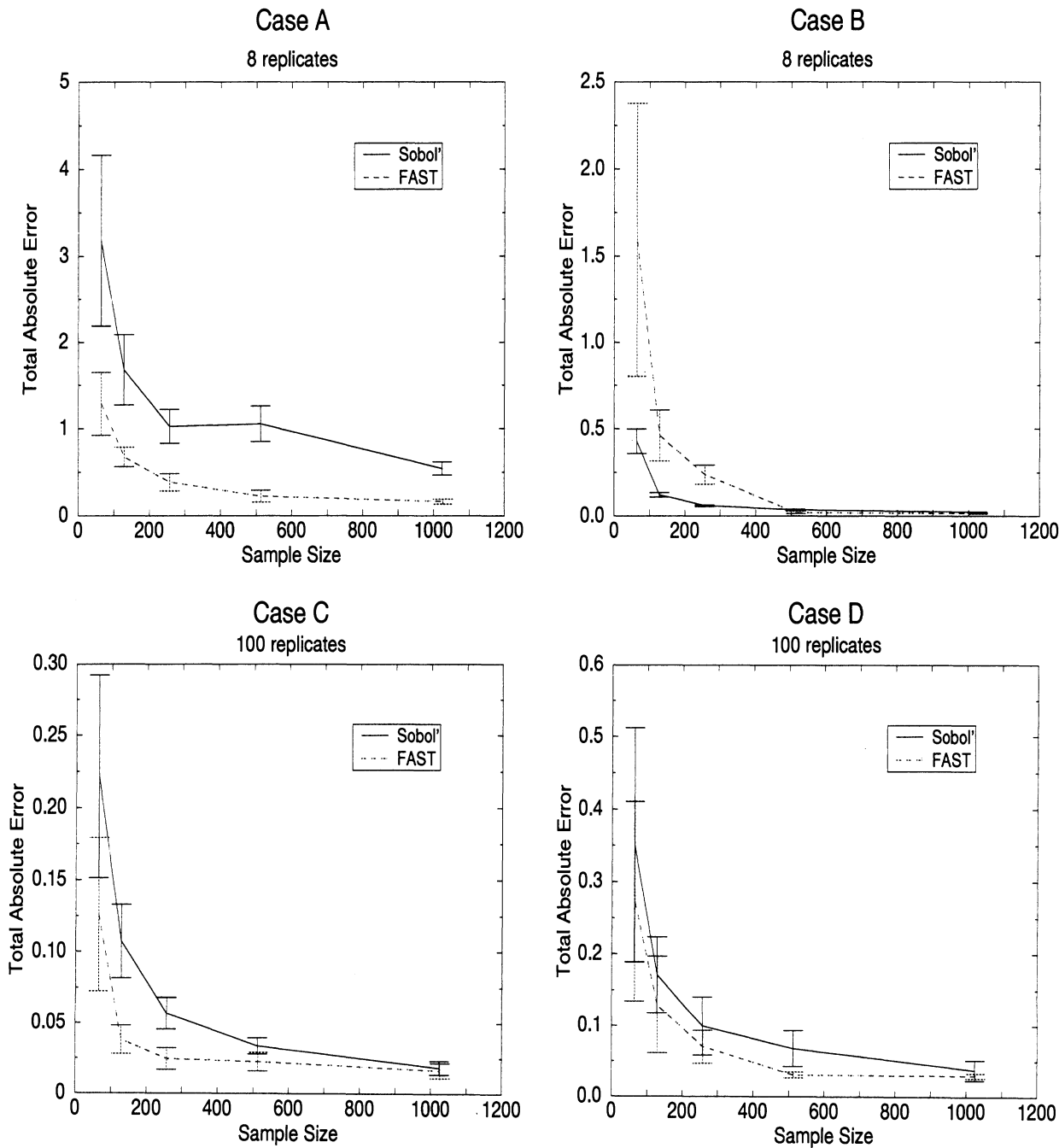

Figure 8. Plots of Means and Error Bars of the Total Absolute Errors Versus Sample Sizes for Case A, Strongly Nonmonotonic Function; Case B, Weak Function; Case C, Factors in Decreasing Order of Importance; and Case D, Factors in Random Order of Importance.

Table 5. Analytical Values of the Partial Variances and the Total Partial Variances and Their Corresponding Sensitivity Indices (shown in bold)

Input factor	Partial variance D_{input}	Total partial variance $D - D_{\sim input}$
d	0	.1405
	0	**.8**
x	.0351	.1756
	.2	**1**

NOTE: $\sim$ denotes "not."

of the 100 bootstrap estimates have been calculated. The set of sample sizes used in the method of Sobol' is 64, 128, 256, 512, 1,024, and 2,048.

For the extended FAST, we repeat the experiment 100 times as done for the g function. The frequencies, ω_i for $i \in \{d, x\}$, are chosen according to the algorithm proposed in Section 4.2. Two sets of results are obtained using the extended FAST, one with the minimum Nyquist criterion—namely $N_s = N_r(2M\omega_{max} + 1)$ (which we refer to as "FAST 1")—and the other with $N_s = N_r(4M\omega_{max} + 1)$ ("FAST 2"). The maximum frequency ω_{max} is chosen such that the sample size used in FAST is as close as possible to the one used by Sobol'. At sample size 64, the S_{Ti}'s of "FAST 2" are not available because the minimum value for ω_{max} is 8, yielding the minimum sample size 129.

Results of this test case for six sample sizes (up to $\sim 2,050$) are shown in Figure 9. The scale and label of the x axis are not the actual values but are presented as groups of the six sample sizes. For example, in the second group the actual sample size for both "FAST 1" and "FAST 2" is 129; that for Sobol' is 128. For factor d [Fig. 9(a)], the estimates of the S_{Ti}'s with "FAST 2" converge to the analytical value quicker than "FAST 1." Moreover, the estimates of "FAST 2" tend to be less variable than those of "FAST 1" as the sample size increases. The ranges of the bootstrap estimates based on Sobol' decrease slowly as the sample size increases, and they are wider than those of both the "FAST 1" and "FAST 2." In summary "FAST 2" yields better estimates than the Sobol' and "FAST 1" methods in terms of precision and variability.

For factor x [see Fig. 9(b)], the ranges of the 100 Sobol' bootstrap estimates are again wider than those of the "FAST 1" and "FAST 2." Both estimates of "FAST 1" and "FAST 2" converge to the true value, but, as for factor d, the estimates of "FAST 1" seem to converge to a value slightly below the analytical value, indicating a possible bias in the estimates. The "FAST 2" method tends to be more robust and precise than "FAST 1." It is also worth noting that, unlike in the method of Sobol', FAST estimates can never be greater than 1.

McKay (1996) commented that the variance-based measures of importance, which use the variance of the conditional expectation of the output—namely, $\text{var}_X[E(Y|X)]$—may not always be effective as indicators of importance and hinted that additional notions of importance might be necessary for assessing uncertainty importance. As shown in Table 5, the S_{Ti}'s offer such additional notions. If considered singularly, both factors d and x appear to be irrelevant to the output variation (the first-order sensitivity indices
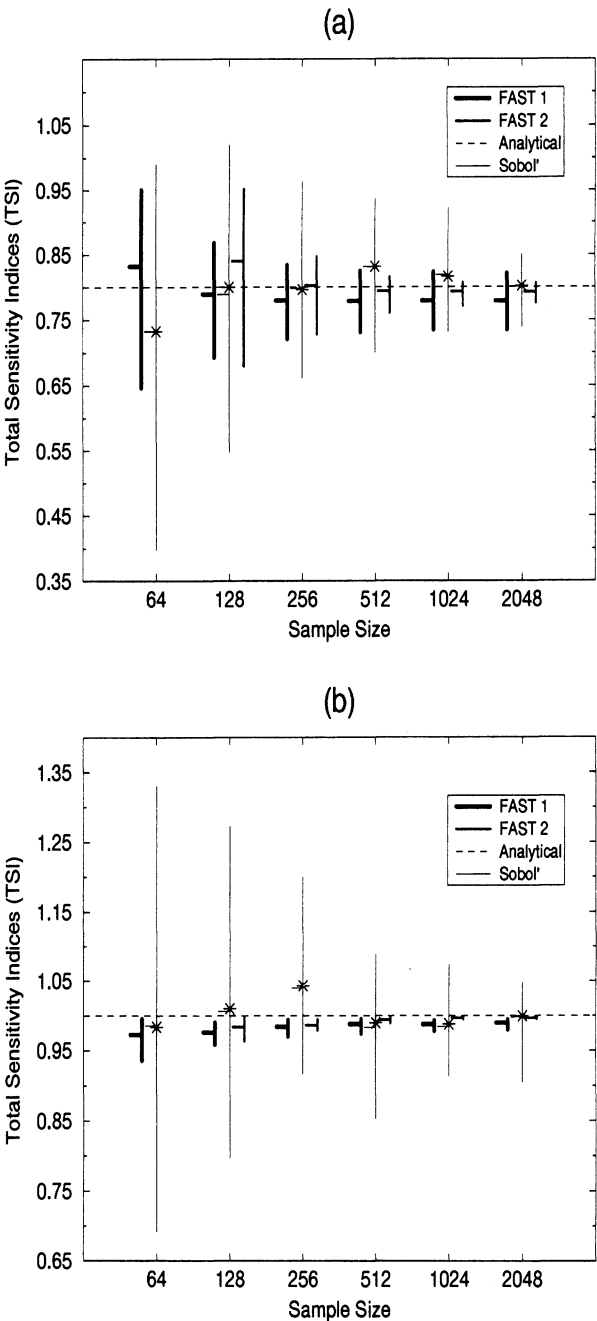
Figure 9. Plots of the Estimated Total Sensitivity Indices (S_{Ti}) Against Various Sample Sizes for (a) Factor d and (b) Factor x. FAST-based S_{Ti}'s are obtained for $N_s = N_r(2M\omega_{max} + 1)$ (FAST 1) and with $N_s = N_r(4M\omega_{max} + 1)$ (FAST 2). For both plots (a) and (b), FAST-based results are based on 100 replicates. The symbols represent the arithmetic means (short horizontal lines) and ranges (long vertical lines). A value of M equal to 4 was selected, and ω_{max} and N_r were chosen by the automated algorithm described in Section 4.2. The same plots also show for comparison the results from the method of Sobol'. The asterisk denotes the estimates based on a single replicate (*), and the range from the bootstrapping procedure (100 estimates) is shown as a thin vertical line. The analytical values of the S_{Ti} of the two factors are $S_{Td} = .8$ and $S_{Tx} = 1.0$ (dashed horizontal lines).

being $S_d = 0$ and $S_x = .2$), although their total effects are $S_{Td} = .8$ and $S_{Tx} = 1.0$. This means that a large interaction occurs between d and x:

$$S_{d,x} = 1 - S_d - S_x = 1 - .0 - .2 = .8. \qquad (28)$$

Table 6. List of Input Factors and Their pdf for the Level E Exercise

Notation	Definition	Distribution	Range	Units
T	Containment time	Uniform	/100, 1,000/	yr
k_I	Leach rate for iodine	Log-uniform	/10^{-3}, 10^{-2}/	yr^{-1}
k_C	Leach rate for Np chain nuclides	Log-uniform	/10^{-6}, 10^{-5}/	yr^{-1}
$v^{(1)}$	Water vel. in geosphere's 1st layer	Log-uniform	/10^{-3}, 10^{-1}/	m/yr
$\ell^{(1)}$	Length of geosphere's 1st layer	Uniform	/100, 500/	m
$R_I^{(1)}$	Retention factor for I (1st layer)	Uniform	/1, 5/	—
$R_C^{(1)}$	Factor to compute ret. coeff. for Np (1st layer)	Uniform	/3, 30/	—
$v^{(2)}$	Water vel. in geosphere's 2nd layer	Log-uniform	/10^{-2}, 10^{-1}/	m/yr
$\ell^{(2)}$	Length of geosphere's 2nd layer	Uniform	/50, 200/	m
$R_I^{(2)}$	Retention factor for I (2nd layer)	Uniform	/1, 5/	—
$R_C^{(2)}$	Factor to compute ret. coeff. for Np (2nd layer)	Uniform	/3, 30/	—
W	Stream flow rate	Log-uniform	/10^5, 10^7/	m^3/yr

Hence, both factors influence the output, even though neither d nor x alone can explain the output variation. This test case confirms the identity of McKay's correlation ratio with Sobol'/FAST first-order indices.

5.3 Level E Test Case

The Level E test case (OECD/NEA PSAC User Group 1989; Saltelli et al. 1993) displays interesting nonmonotonic features that are suitable for testing the extended FAST and for comparing it with the method of Sobol'. Level E case study simulates the transport of radionuclides from an underground disposal vault containing nuclear waste up to man, by way of migration through a system of natural and engineered barriers. The main barrier considered in the model is the geosphere itself, which includes a two-layer pathway, where nuclide dispersion, advection, retention, and radioactive decay are considered. After a delay representing primary containment failure, the release of radionuclides to the geosphere depends only on leach rate and inventory.

The isotope ^{129}I and the decay chain $^{237}Np \rightarrow ^{233}U \rightarrow ^{229}Th$ are the migrating species. The model has a total of 33 factors, 12 of which are taken as uncertain; the pdf's that are used to characterize their uncertainties are given in Table 6. The core of the model is a set of partial differential equations that describes the nuclide migration in the geosphere; to give an example, for ^{233}U the equation is

$$R_U^{(k)} \frac{\partial F_U^{(k)}}{\partial t} + v^{(k)} \frac{\partial F_U^{(k)}}{\partial x} - v^{(k)} d^{(k)} \frac{\partial^2 F_U^{(k)}}{\partial x^2}$$
$$= -\lambda_U R_U^{(k)} F_U^{(k)} + \lambda_N R_N^{(k)} F_N^{(k)},$$

where U stands for ^{233}U and N for ^{237}Np, (k) refers to geosphere layer number (1 or 2), R_i is the retardation coefficient for nuclide i (dimensionless), $F_i(x,t)$ is the flow (amount transported per unit time) of nuclide i in the geosphere at position x and time t (mols/yr), v is the water travel velocity in the geosphere (m/yr), d is the dispersion length in the geosphere (m), and λ_i is the decay constant for nuclide i (yr^{-1}). The geosphere flow is assumed to enter a stream, which is used for drinking water. The dose received depends on the ratio of the drinking-water consumption and the stream-flow rate. The dose [in (Sv/yr)]

arising from nuclide i is computed by

$$\text{dose}_i(t) = \beta_i \frac{w}{W} F_i^{(2)}(l^{(2)}, t), \quad i = {}^{129}I, {}^{237}Np, {}^{233}U, {}^{229}Th,$$

where β_i is a dose conversion factor and is assumed fixed, $F_i^{(2)}(l^{(2)}, t)$ is the flow of nuclide i at the end of the second layer (the output to the biosphere), w denotes the individual drinking-water requirement and is taken to be .73 m^3/yr, and W and $l^{(k)}$ are defined in Table 6. The output considered in the discussion to follow is the total annual dose $\sum_i \text{dose}_i(t)$.

The S_{Ti}'s computed using the method of Sobol' are plotted in Figure 10(a) as a function of time. It can be seen that the four most influential factors are, in order of importance, the water velocity in the first layer ($v^{(1)}$), the stream-flow rate (W), the length of the first layer ($l^{(1)}$), and, finally, the retardation factor for Np chain nuclides in the first layer ($R_N^{(1)}$), which becomes important after 10^5 years.

Even for this test case the bootstrap technique has been applied. Plots of the arithmetic means and the ranges of 100 bootstrap S_{Ti} estimates against time at sample sizes 8,192 and 1,024 are shown in Figure 11, (a) and (b), respectively. The plots refer to the factor $v(1)$. It can be seen from these figures that the 100 bootstrap estimates at 1,024 sample size are more erratic than those obtained with sample size 8,192; the ranges are generally wider, particularly at times below 10^5 years and above $3 \cdot 10^6$ years. The same happens for the other factors. This suggests that neither 1,024 runs nor 8,192 runs are sufficient to give reliable information about the ranking of importance of the factors.

For FAST, 100 estimates have been obtained for the factor $v(1)$ at sample size 1,025 ($N_r = 1, \omega_i = 128$, and $M = 4$) and at sample size 257 ($N_r = 1, \omega_i = 32$, and $M = 4$). Results are shown in Figure 12, (a) and (b). The estimates at sample size 1,025 appear to be more stable than those of Sobol' at 8,192; this implies that FAST gives consistent estimates of the S_{Ti}'s at lower sample size. Results at sample size 257 show that FAST can yield consistent estimates at even lower sample size; therefore, the S_{Ti} estimates for all the factors at sample size 257 have been plotted in Figure 10(b). At this low sample size, FAST is capable of pinpointing the four most important factors consistently with Sobol'.
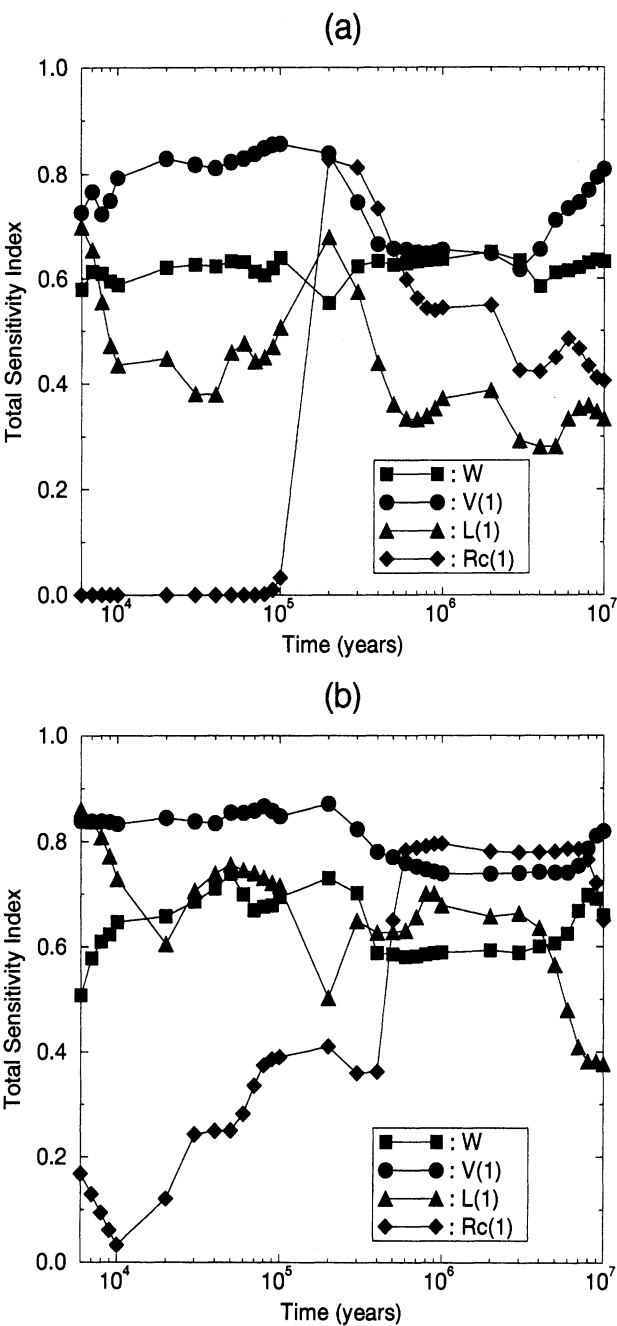
(a)

(b)

Figure 10. Plots of the S_{Ti} Estimates for all Factors Against Time Using (a) Sobol' Method at Sample Size 8,192 and (b) FAST at Sample Size 257.

Another important feature of the FAST method should be emphasized. When using the method of Sobol' there is no difference, from the point of view of the computational cost, between a first-order term $\hat{S}_i$ and a total-effect index $\hat{S}_{Ti}$. The formulas involved in their computation are formally identical (see Sobol' 1993), although different samples are needed to compute either an $\hat{S}_i$ term or an $\hat{S}_{Ti}$ one. In other words, the test model must be executed $(n+1)N_s$ times (where n is the number of factors and N_s is the sample size) for computing any of the $\hat{S}_i$'s given in Figure 13(a) and another $(n+1)N_s$ times for computing all the $\hat{S}_{Ti}$'s given in Figure 10(a).

FAST is capable of yielding both the main- and the total-effect index for a certain factor from the same set of model evaluations. Indeed, by adding together the spectral components in $[1, \omega_i/2]$ and at frequencies $\omega_i, 2\omega_i, \ldots, M\omega_i$, the quantities D_{-i} and D_i, respectively, can be estimated. This means that, besides the $\hat{S}_{Ti}$'s given in Figure 10(b), we can also obtain, at no extra computational cost, all the $\hat{S}_i$'s shown in Figure 13(b).

From the comparison of results given in Figures 10(b) and 13(b), the predominance of the higher-order terms is evident. The $\hat{S}_i$'s stay below .1 for almost the entire time span, with local maxima at about .2. The $\hat{S}_{Ti}$'s are much higher and often close to 1. Hence, it can be said that the
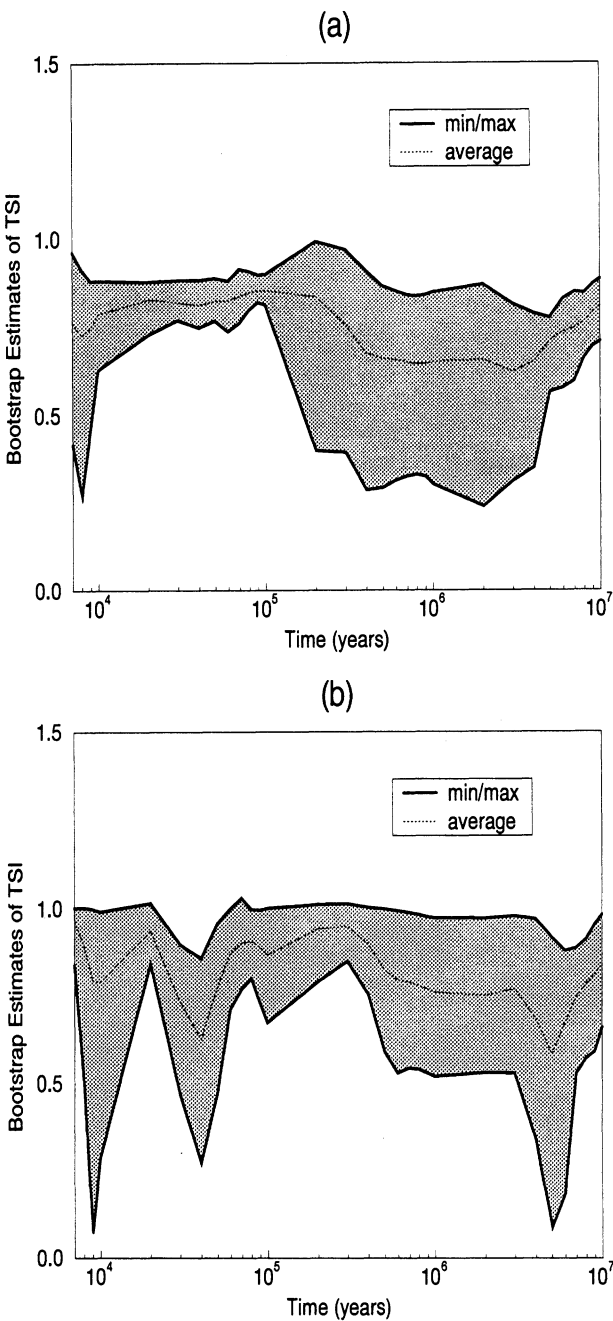
(a)

(b)

Figure 11. Plot of the Averages and Ranges of 100 Sobol' Bootstrap Estimates of S_{Ti} for Factor v(1) Against Time at Sample Size (a) 8,192 and (b) 1,024.
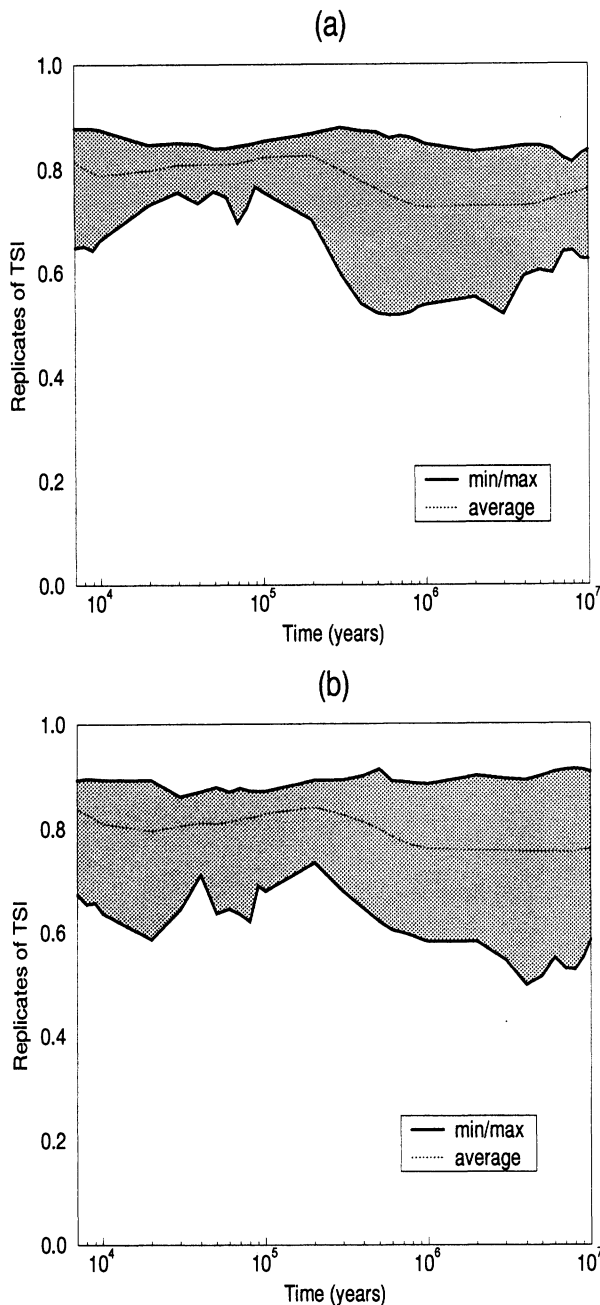
(a)

(b)

Figure 12. Plot of the Averages and Ranges of 100 FAST Estimates of S_{Ti} for Factor $v(1)$ Against Time at Sample Size (a) 1,025 and (b) 257.

factors' influence is mostly due to interaction terms rather than to linear effects.

Level E shows that the relevance of the interaction terms is not just an artifact of made-on-purpose analytic mathematical functions.

6. CONCLUSIONS

We have shown how the classic (main-effect) FAST coefficients are identical to Sobol' indices of the first order and that these in turn are equal to the so-called importance measures or correlation ratios introduced by several investigators. All these measures are estimates of Equation (1). It is hence a matter of preference which term is used to define them.

Furthermore, the total sensitivity indices, either in the implementation of Sobol' or in that based on the extended FAST introduced here, are especially suited for a quantitative, model-independent global sensitivity analysis. The method also allows a rigorous but intuitive display of the results (such as the pie-chart in Fig. 1). Alternative global methods, based on correlation or regression coefficients such as SRC, are model dependent, and hence often they may only offer a qualitative picture of model sensitivity. Furthermore, they may fail altogether for nonmonotonic models. To overcome this limitation the user of those methods can resort to the manual or automated investigation of scatterplots (Kleijnen and Helton 1998).
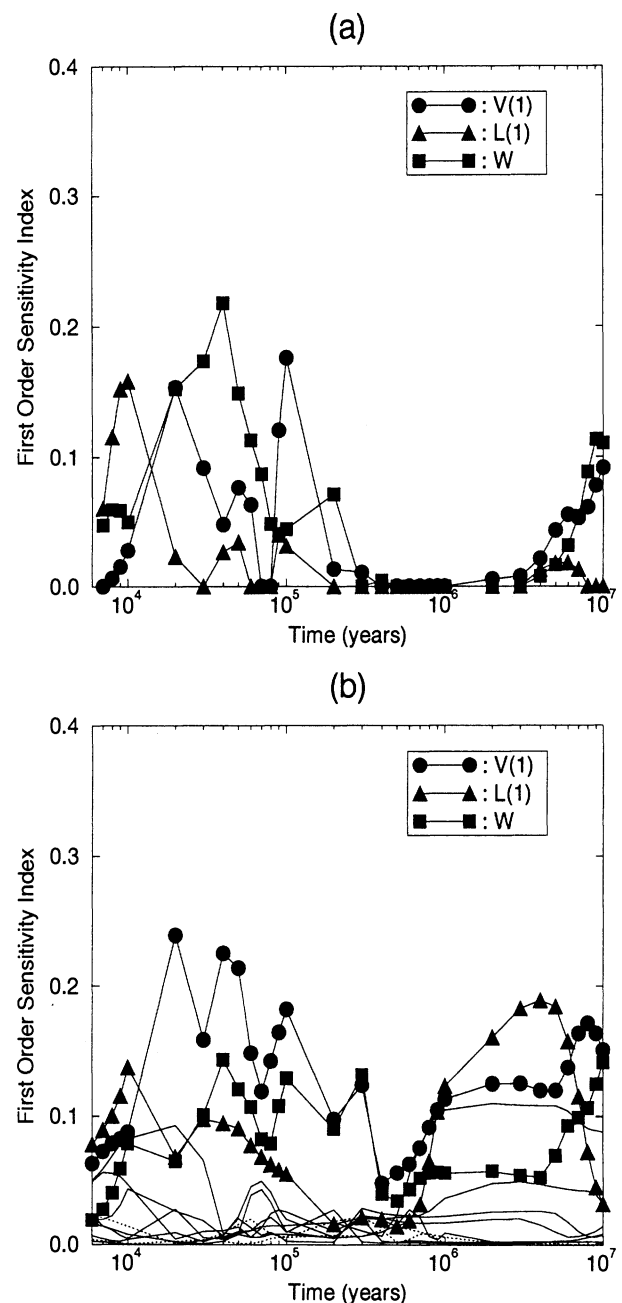
(a)

(b)

Figure 13. Plot of the First-Order Estimates Against Time Using (a) Sobol' at Sample Size 8,192 for the Three Most Important Factors [$v(1)$, $l(1)$, and W] and (b) FAST at Sample Size 257 for all Factors.

Global methods for reliability analysis, such as the first-order reliability method (FORM, Cawlfield and Wu 1993), offer a valid alternative for the problem setting in which only a specific (e.g., high-risk) space of the input factors is of interest.

The total indices are computationally more expensive than both the correlation/regression measures and the screening tests such as that of Morris (1991). The Morris method is especially effective in its capacity to discriminate, at low sample size, among noninfluential, linearly influential, and influential by way of either nonlinear or interaction effects. The total sensitivity indices offer something more at a higher price—that is, the capacity to rank quantitatively the factors, based on all effects, whether they are additive or not.

The computational cost of an SA coincides with the cost of running the model f because usually the cost of elaborating the model evaluations to extract the sensitivity measures is negligible. When we move from a screening method to one of the variance-based tests addressed here, we usually shift from a computational cost in the range from tens to hundreds to one in the range from hundreds to thousands model executions. Whether this is affordable or not depends on the computational cost of a single run of the model. The ever-increasing power of computers would suggest that global methods may also become affordable for a large class of models.

The method of Sobol' was, up till now, the only procedure that allowed the computation of the total sensitivity indices; the extended FAST is now a convenient alternative technique. There is another important implication related to the use of the sensitivity indices that has not been discussed so far; the total indices are in fact only one among the possible ways of combining elementary (main or otherwise) effects. Sobol' (1993) tackled the problem of ascertaining if a given subset of the input factors could account for most of the output variance so that the others could be "frozen" at their midpoint. This approach was linked to an optimization problem. The generalized formulation of variance decomposition is $D = D_{\mathbf{v}} + D_{\mathbf{w}} + D_{\mathbf{vw}}$, where $\mathbf{v}$ and $\mathbf{w}$ are any two complementary subsets of $\mathbf{x}$. One implication of this feature is that one can apportion the output variation to groups of factors (e.g., near-field, far-field, biosphere in the Level E example) or to factors of different logical types. This can be done either via the extended FAST or the Sobol' approach, and the computational cost is lower than for computing all indices for all factors individually.

From the results shown in this article it seems that the extended FAST (searching in the space of the frequencies) is generally more efficient than the method of Sobol' (searching the space K^n), thus confirming the strategy of the classic FAST developers of tackling the sensitivity problem in the transformed frequency space.

Both the method of Sobol' and the extended FAST have a common limitation; that is, they cannot estimate all the S_{Ti}'s with a single set of model evaluations, but several samples equal to the number of factors are needed. Unlike Sobol', however, the extended FAST approach offers,

for the same set of model evaluations, both the first-order indices and the total ones.

APPENDIX A: ALIASING AND SAMPLE SIZE

We describe the relationship between aliasing and sample size in the classic (Cukier et al. 1973) FAST.

In FAST, the model f must be evaluated at N_s equally spaced sample points along the closed path in the interval $(-\pi, \pi)$. Aliasing is the unwanted process by which a discrete sampling adds frequency information that has escaped the analysis back into the explored frequency range. The sequence of sampled values is $y_k = f(s_k)$ with $s_k = \pi/N_s(2k - N_s - 1), \forall\, k = 1, 2, \ldots, N_s$, so that $s_{N_s} = -s_1 = \pi(1 - (1/N_s))$. It is useful to choose N_s odd to include also the point $s = 0$ in the symmetric set of samples.

Let $\Delta s = (s_{N_s} - s_1)/(N_s - 1) = (2\pi/N_s)(N_s - 1)/(N_s - 1) = (2\pi/N_s)$ denote the distance between consecutive samples. The expansion (11) becomes

$$y_k = f(s_k) = \sum_{j \in \bar{\mathcal{Z}}} \{A_j \cos j s_k + B_j \sin j s_k\},$$

where

$$\bar{\mathcal{Z}} = \left\{ -\frac{N_s - 1}{2}, \ldots, -1, 0, 1, \ldots, \frac{N_s - 1}{2} \right\} \subset \mathcal{Z}$$

and

$$
\begin{aligned}
A_j &= \frac{1}{N_s} \sum_{k=1}^{N_s} f(s_k) \cos j s_k \\
B_j &= \frac{1}{N_s} \sum_{k=1}^{N_s} f(s_k) \sin j s_k, \qquad j \in \bar{\mathcal{Z}}. \quad \text{(A.1)}
\end{aligned}
$$

With N_s values in s domain, we will evidently be able to produce no more than N_s independent values for A_j and B_j in the frequency domain. For any choice of N_s equally spaced points in $(-\pi, \pi)$, there is a special frequency $\omega_{N_y} = 2\pi \cdot (1/2\Delta s)$, called the *Nyquist critical frequency*. It allows the study of the spectral components that lie inside the frequency range $(-\omega_{N_y}, \omega_{N_y})$. By making explicit the dependency of Δs on N_s, we have

$$\omega_{N_y} = \frac{N_s}{2}. \qquad \text{(A.2)}$$

The frequency resolution $d\omega$ is the distance between consecutive points in the frequency domain. From Equation (A.2), we have $d\omega = 1$.

A problem may occur if the model f, in the frequency space, contains harmonic components that lie out of the range $(-\omega_{N_y}, \omega_{N_y})$. In this case, it turns out that any of these components is *aliased* (falsely translated) into that range by the very act of discrete sampling. Ways to overcome aliasing are (1) to estimate the bandwidth of the function $f(s)$ and (2) to sample at a rate sufficiently high to increase the Nyquist critical frequency up to capture the entire bandwidth by an appropriate choice of $\{\omega_i\}; i = 1, 2, \ldots, n$.

Naturally, the higher the sampling rate Δs, the larger is N_s, the base sample size. Let us assume that we are using a set of integer frequencies $\{\omega_1, \omega_2, \ldots, \omega_n\}$. Then, the frequency components of $f(s)$ at $\{p_1\omega_1, p_2\omega_2, \ldots, p_n\omega_n\}$, $\forall \ p_1, p_2, \ldots, p_n \in \{1, \ldots, +\infty\}$, can be used to compute the partial variances due to each factor, and the entire frequency axis can be explored to obtain the total variance.

Normally, the spectral components decrease as the p_i's increase, and we expect most of the information to be accounted for by the low p values. To keep the sample size low, we assume $f(s)$ to be approximately bandwidth limited in $(-M\omega_{\max}, M\omega_{\max})$, where $\omega_{\max} = \max\{\omega_1, \omega_2, \ldots, \omega_n\}$ and M is an integer number indicating how many higher harmonics are considered—that is, the maximum value for the p_i's. Generally M is taken to be 4 or 6.

Because ω_{N_y} has to be greater than $M\omega_{\max}$ and given (A.2), the minimum number of sample points required in the computation of a given partial variance is $N_s = 2M\omega_{\max} + 1$.

APPENDIX B: THE PROBLEM OF INTERFERENCES

We describe in this subsection the problem of selecting frequencies while avoiding interference in the classic FAST, following Cukier et al. (1978).

The use of integer frequencies implies some limitation when evaluating the $\hat{D}_i$'s. In a case with only two factors x_1 and x_2 and their associated frequencies ω_1 and ω_2, there exists at least a combination of harmonic indices, p_1 and p_2, such that $p_1\omega_1 = p_2\omega_2$. The spectrum at frequency $p_1\omega_1$ contains information that mixes together the contributions due to both $\hat{D}_1$ and $\hat{D}_2$, and there is no way to separate them. This interference could lead to overestimating all the $\hat{D}_i$'s, but the error may be kept low if we let interference occur at high frequencies only, where spectral information is smaller.

In a model with several factors the linear combinations among the $\{\omega_i\}$'s may produce interference. We adopt the recursive algorithm proposed by Cukier et al. (1975) to obtain a linearly independent set of frequencies such that

$$\sum_{i=1}^{n} a_i\omega_i \neq 0 \quad \text{for} \quad \sum_{i=1}^{n} |a_i| \leq M' + 1, \qquad \text{(B.1)}$$

where the a_i's are relative integer numbers and M' is a positive integer at our choice.

The set of frequencies is said to be free of interferences "up to order M'." Normally it is sufficient to consider $M' = M$ because it is believed that further harmonic effects are negligible.

The problem of choosing the frequencies becomes more and more difficult as the number of factors increases. In conclusion, the building blocks for the sensitivity measure, given in (13) and (14), can be rewritten as

$$\hat{D}_i = 2\sum_{p=1}^{M} \Lambda_{p\omega_i}, \quad \hat{D} = 2\sum_{j=1}^{(N_s-1)/2} \Lambda_j,$$

where $\Lambda_j = A_j^2 + B_j^2$ and A_j and B_j are given in (A.1).

APPENDIX C: SYMMETRY PROPERTIES

We describe the use of the symmetry properties in the classic FAST, following Koda et al. (1979).

The investigation of the symmetry properties of a 2π periodic curve may be helpful in reducing the number of model evaluations.

By using a set $\{\omega_i\}$ of odd integer frequencies, the function $f(s)$ shows a symmetry around $s = \pm\pi/2$. We may then restrict the range of integration from $(-\pi, \pi)$ to $(-\pi/2, \pi/2)$ halving the number of model evaluations required (indicated in the following as N_s'). The frequencies proposed by Cukier et al. (1975) are, actually, odd integers, and therefore they may be suitably used for this purpose. Koda et al.'s procedure consists of sampling the function $f(s)$ in $(-\pi/2, \pi/2)$ including $s = 0$ by using $s_k = \pi/2((2k - N_s' - 1)/N_s'), \forall \ k = 1, 2, \ldots, N_s'$, where $N_s' = (N_s + 1)/2$. Δs is the same as before, and this is also true for ω_{N_y}. The frequency resolution is now $d\omega = 2$, and the new expressions for the Fourier coefficients A_j and B_j are

$$A_j = \begin{cases} \frac{1}{N_s'}\left\{f(s_{N_o}) + \sum_{q=1}^{N_q}[f(s_{N_o+q}) + f(s_{N_o-q})] \right. \\ \left. \times \cos\left(j\frac{\pi}{N_s'}q\right)\right\} & \text{if } j \text{ even} \\ 0 & \text{if } j \text{ odd} \end{cases}$$

$$B_j = \begin{cases} 0 & \text{if } j \text{ even} \\ \frac{1}{N_s'}\left\{\sum_{q=1}^{N_q}[f(s_{N_o+q}) - f(s_{N_o-q})] \right. \\ \left. \times \sin\left(j\frac{\pi}{N_s'}q\right)\right\} & \text{if } j \text{ odd,} \end{cases}$$

where $N_q = (N_s' - 1)/2$ and $N_o = (N_s' + 1)/2$.

REFERENCES

Abramowitz, M., and Stegun, I. A. (1970), *Handbook of Mathematical Functions*, New York: Dover Publications.

Archer, G., Saltelli, A., and Sobol', I. M. (1997), "Sensitivity Measures, ANOVA like Techniques and the Use of Bootstrap," *Journal of Statistical Computation and Simulation*, 58, 99–120.

Box, G. E. P., Hunter, W. G., and Hunter, J. S. (1978), *Statistics for Experimenters: An Introduction to Design, Data Analysis and Model Building*, New York: Wiley.

Cacuci, D. G. (1981a), "Sensitivity Theory for Nonlinear Systems. I. Nonlinear Functional Analysis Approach," *Journal of Mathematical Physics*, 22, 2794–2802.

——— (1981b), "Sensitivity Theory for Nonlinear Systems. II. Extensions to Additional Classes of Response," *Journal of Mathematical Physics*, 22, 2803–2812.

Campolongo, F., and Saltelli, A. (1997), "Sensitivity Analysis of an Environmental Model; a Worked Application of Different Analysis Methods," *Reliability Engineering and System Safety*, 52, 49–69.

Cawlfield, J. D., and Wu, M.-C. (1993), "Probabilistic Sensitivity Analysis for One-Dimensional Reactive Transport in Porous Media," *Water Resources Research*, 29, 661–672.

Cotter, S. C. (1979), "A Screening Design for Factorial Experiments With Interactions," *Biometrika*, 66, 317–320.

Cukier, R. I., Fortuin, C. M., Shuler, K. E., Petschek, A. G., and Schaibly, J. H. (1973), "Study of the Sensitivity of Coupled Reaction Systems to Uncertainties in Rate Coefficients. I. Theory," *The Journal of Chemical Physics*, 59, 3873–3878.

Cukier, R. I., Levine, H. B., and Shuler, K. E. (1978), "Nonlinear Sensitivity Analysis of Multiparameter Model Systems," *Journal of Computational Physics*, 26, 1–42.

Cukier, R. I., Schaibly, J. H., and Shuler, K. E. (1975), "Study of the Sensitivity of Coupled Reaction Systems to Uncertainties in Rate Coefficients. III. Analysis of the Approximations," *The Journal of Chemical Physics*, 63, 1140–1149.

Helton, J. C. (1993), "Uncertainty and Sensitivity Analysis Techniques for Use in Performance Assessment for Radioactive Waste Disposal," *Reliability Engineering and System Safety*, 42, 327–367.

Homma, T., and Saltelli, A. (1996), "Importance Measures in Global Sensitivity Analysis of Nonlinear Models," *Reliability Engineering and System Safety*, 52, 1–17.

Hora, S. C., and Iman, R. L. (1986), "A Comparison of Maximum/Bounding and Bayesian/Monte Carlo for Fault Tree Uncertainty Analysis," Technical Report SAND85-2839, Sandia National Laboratories, Sandia, NM.

Iman, R. L., and Hora, S. C. (1990), "A Robust Measure of Uncertainty Importance for Use in Fault Tree System Analysis," *Risk Analysis*, 10, 401–406.

Ishigami, T., and Homma, T. (1990), "An Importance Quantification Technique in Uncertainty Analysis for Computer Models," in *Proceedings of the ISUMA '90, First International Symposium on Uncertainty Modelling and Analysis, Univ. of Maryland, USA*, New York: IEEE Computer Society, pp. 398–403.

Kleijnen, J. P. C., and Helton, J. C. (1998), "Statistical Analyses of Scatterplots to Identify Important Factors in Large-Scale Simulations," technical report, Sandia National Laboratories, Sandia, NM.

Koda, M., McRae, G. J., and Seinfeld, J. H. (1979), "Automatic Sensitivity Analysis of Kinetic Mechanisms," *International Journal of Chemical Kinetics*, 11, 427–444.

Krzykacz, B. (1990), "SAMOS: A Computer Program for the Derivation of Empirical Sensitivity Measures of Results From Large Computer Models," Technical Report GRS-A-1700, Gesellschaft fuer Reaktor Sicherheit (GRS) MbH, Garching, Germany.

Liepmann, D., and Stephanopoulos, G. (1985), "Development and Global Sensitivity Analysis of a Closed Ecosystem Model," *Ecological Modelling*, 30, 13–47.

McKay, M. D. (1996), "Variance-Based Methods for Assessing Uncertainty Importance in NUREG-1150 Analyses," Report LA-UR-96-2695, Los Alamos National Laboratory, Los Alamos, NM.

Morris, M. D. (1991), "Factorial Sampling Plans for Preliminary Computational Experiments," *Technometrics*, 33, 161–174.

Oblow, E. M., Pin, F. G., and Wright, R. Q. (1986), "Sensitivity Analysis Using Computer Calculus: A Nuclear Waste Isolation Application," *Nuclear Science and Engineering*, 94, 46–56.

OECD/NEA PSAC User Group (1989), "PSACOIN Level E Intercomparison, an International Code Intercomparison Exercise on a Hypothetical Safety Assessment Case Study for Radioactive Waste Disposal Systems," technical report, OECD/NEA, Paris.

Pierce, T. H., and Cukier, R. I. (1981), "Global Nonlinear Sensitivity Analysis Using Walsh Functions," *Journal of Computational Physics*, 41, 427–443.

Rabitz, H. (1989), "System Analysis at Molecular Scale," *Science*, 246, 221–226.

Sacks, J., Welch, W. J., Mitchell, T. J., and Wynn, H. P. (1989), "Design and Analysis of Computer Experiments," *Statistical Science*, 4, 409–435.

Saltelli, A., Andres, T. H., and Homma, T. (1993), "Sensitivity Analysis of Model Output: An Investigation of New Techniques," *Computational Statistics and Data Analysis*, 15, 211–238.

——— (1995), "Sensitivity Analysis of Model Output. Performance of the Iterated Fractional Factorial Design (IFFD) Method," *Computational Statistics and Data Analysis*, 20, 387–407.

Saltelli, A., and Bolado, R. (1998), "An Alternative Way to Compute Fourier Amplitude Sensitivity Test (FAST)," *Computational Statistics and Data Analysis*, 26, 445–460.

Saltelli, A., and Scott, M. (1997), "The Role of Sensitivity Analysis in the Corroboration of Models and its Links to Model Structural and Parametric Uncertainty," *Reliability Engineering and System Safety* (Special Issue on Sensitivity Analysis of Model Output), 52, 1–4.

Saltelli, A., and Sobol', I. M. (1995), "About the Use of Rank Transformation in Sensitivity Analysis of Model Output," *Reliability Engineering and System Safety*, 50, 225–239.

Schaibly, J. H., and Shuler, K. E. (1973), "Study of the Sensitivity of Coupled Reaction Systems to Uncertainties in Rate Coefficients. Part II, Applications," *Journal of Chemical Physics*, 59, 3879–3888.

Sobol', I. M. (1993), "Sensitivity Analysis for Nonlinear Mathematical Models," *Mathematical Modeling & Computational Experiment*, 1, 407–414 [translation of Sobol' (1990), "Sensitivity Estimates for Nonlinear Mathematical Models," *Matematicheskoe Modelirovanie*, 2, 112–118 (in Russian)].

Turanyi, T. (1990), "Sensitivity Analysis of Complex Kinetic Systems. Tools and Applications," *Journal of Mathematical Chemistry*, 5, 203–248.

Weyl, H. (1938), "Mean Motion," *American Journal of Mathematics*, 60, 889–896.